



ISSN: 2348-2079

International Journal of Intellectual Advancements and Research in Engineering Computations (IJAREC)

IJAREC | Vol.11 | Issue 4 | Oct - Dec -2023

www.ijarec.com

DOI :<https://doi.org/10.61096/ijarec.v11.iss4.2023.39-58>

Research

Leveraging Machine Learning for Predictive Modeling in 3D Printing of Composite Materials: A Comparative Study



Nitesh Kumar Ramancha^{1*} and Satyanarayana Ballamudi²

¹ *Sr. SAP Consultant, SAP, TX, USA*

² *ERP Analyst / Developer Lead, Lennox International Inc., TX, USA*

* Author for Correspondence: Nitesh Kumar Ramancha

Email: nkr112024@gmail.com

	Abstract
Published on: 28 Nov 2023	<p>This study explores how additive manufacturing, commonly referred to as 3D printing, has transformed a number of industries by making it possible to precisely create intricate structures. By providing improved mechanical qualities and adaptability for a variety of uses, the incorporation of composite materials into 3D printing has further increased its potential. Composites can be engineered to attain particular features like improved strength, stiffness, or heat resistance. Composites are created by combining two or more different materials. When using composite materials in 3D printing, reinforcing agents like carbon fibres, glass fibres, or ceramics are usually combined with a matrix material, like thermoplastics. These reinforcements improve the material's performance, enabling the production of parts that are both lightweight and durable. The research into composite 3D printing aims to improve material properties, reduce costs, and expand the range of applications, driving innovation and optimization in material science and engineering. The prediction of tensile strength (MPa) in 3D printing by evaluating the influence of key process parameters, including printing speed (mm/s), nozzle temperature (°C), and filler material percentage (%). Three regression models for machine learning The link between the input parameters and the output tensile strength is examined using Support Vector Machines (SVM), Random Forest Regression, and Linear Regression. The best predictive tool for maximising the mechanical qualities of printed materials is identified by comparing the performance of each model; this tool may be used to raise the calibre and dependability of 3D-printed parts.</p>
Published by: DrSriram Publications	
2023 All rights reserved.  Creative Commons Attribution 4.0 International License.	
	<p>Keywords: 3D printing of composite materials, Linear Regression, Random Forest Regression, Support Vector Machines (SVM).</p>

INTRODUCTION

Dentistry has been transformed by 3D printing, especially in the production of personalised implants, surgical guides, aligners, and restorations. This innovative technology makes use of a variety of composites and polymers, each specifically designed to address particular dental requirements. The materials utilised in dental 3D printing are examined in this paper, with an emphasis on orthodontic applications. 3D-printed crowns, bridges, surgical guides, removable prostheses, and aligners are noteworthy innovations. Modern manufacturing processes in a variety of dental professions, including prosthetics, periodontology, oral and dental surgery, implantology, orthodontics, and regenerative dentistry, are made possible by the ongoing development of innovative materials, including ecologically friendly solutions.

To ensure their clinical safety, new materials such as PLA infused with nanohydroxyapatite and PMMA reinforced with nanodiamonds need more research. All things considered, 3D printing in dentistry has a bright future ahead of it, with the potential to revolutionise patient care and treatment results. [1]the description of composite materials made from lightweight-poly(lactic acid) (LW-PLA) and poly(lactic acid) (PLA) filaments. The characteristics of composite constructions made using dual-nozzle fused-deposition modelling (FDM) 3D printing are examined. In particular, the study investigates cube-shaped structures, some of which have PLA and LW-PLA filament layers that alternate. Analyzing the effects of mixing these two materials on the mechanical and physical characteristics of the composites is the goal. The findings could offer valuable insights into applications requiring lightweight yet durable components, such as in manufacturing and design. This work adds to the expanding knowledge base on utilizing 3D printing technology for developing advanced composite materials. [2]3D printing parameters for composite filaments made from natural fibers, particularly flax, combined with poly(lactic acid) (PLA).

The growing demand for composite fiber materials in the automotive and machinery industries underscores the importance of this research. Using Fused Deposition Modeling (FDM), the authors developed a novel composite filament and conducted an in-depth evaluation of its mechanical properties. To refine the 3D printing process, the study applied Taguchi's L27 orthogonal array, enabling a structured assessment of key characteristics include occupancy ratios, nozzle speed, infill patterns, and layer thickness. Tensile and impact tests were used to test mechanical performance in accordance with American Society for Testing and Materials (ASTM) guidelines. The findings demonstrated the crucial role that layer thickness plays in tensile characteristics, and particular values were found to maximise impact resistance and tensile strength. This work advances sustainable manufacturing methods by offering insightful information about using natural fibres in composite materials for 3D printing. [3] Continuous fiber-reinforced thermoset composites (CFRPCs) were robotically 3D printed, demonstrating the cost-effectiveness of 3D printing for quick prototyping and composite material modification. It underscores the advantages of integrating multi-axis robotic systems into the printing process, which enhance motion precision, design versatility, and scalability in manufacturing. A robot-assisted manufacturing platform is presented, accompanied by a digital workflow specifically designed for 3D printing UV-curable CFRPCs. The research establishes a transferable protocol that includes coordinate computation, trajectory planning, and validation processes, enabling the creation of composite samples on both flat and curved surfaces. Additionally, the study demonstrates the ability to print on substrates with unknown geometries using laser-based 3D scanning.

These methods and workflows are adaptable to a broad range of feedstock materials and robotic systems, marking a notable advancement in 3D-printed CFRPC technology and opening doors to further innovations in the field. [4]Three-dimensional (3D) printing technology's incorporation of carbon fibre and polymer matrix composites highlights the exceptional advantages of fusing the lightweight, strong, and long-lasting qualities of carbon fibre with polymer matrices. This collaboration opens up new avenues for creative designs and production uses in a variety of sectors, including medical devices, aircraft, automotive, and space exploration. The conversation is on 3D printing material innovations, assessing the state of the art and prospects for these technologies in the future. It discusses the difficulties of integrating carbon fiber-polymer composites into the 3D printing process while highlighting their special qualities and benefits. The article is a vital resource for materials science and engineering professionals and researchers, providing a comprehensive overview of the current state, advantages, challenges, and opportunities.[5]3D printing techniques, Using stereolithography and extrusion to create multipurpose polymer composites . It highlights the innovative integration of traditional additive manufacturing polymers like PEGDA with biomedical polymers such as PVA. Additionally, the inclusion of carbon nanostructures, such as nano diamonds and graphene nano plates, along with conductive polymers like PEDOT and PANI, enables the creation of objects with customized functional properties.

These advanced materials are especially useful in biomedical applications, including the fabrication of scaffolds that promote cell growth and proliferation. The study also explores the development of soft electrodes for use in organic compound sensors and electrocardiogram monitoring systems, offering real-time monitoring capabilities. Overall, it underscores the potential of these cutting-edge 3D printing methods to create versatile and functional polymer composites for many different applications. [6]the creation and improvement of

biomass–fungi composite materials using fungal hyphae and particles of agricultural residue. These materials have a lot of promise for use in sectors like construction, furniture, and packaging. The study highlights 3D printing as a cutting-edge manufacturing process that offers a contemporary substitute for conventional moulding techniques. But there are still issues to be resolved, such as attaining exact geometric correctness and dealing with height shrinking after printing. The study presents the innovative idea of using ionic crosslinking in the 3D printing process to get around these problems. To improve the quality of printed samples, this technique uses calcium chloride as a crosslinking agent and sodium alginate as a hydrogel. The study looks at how ionic crosslinking affects the physical characteristics of the composite materials and the quality of 3D-printed outputs. Results reveal that increasing sodium alginate concentration improves geometric accuracy, minimizes height shrinkage, and enhances the texture and cohesiveness of the biomass–fungi mixtures. [7] 3D composite printing, focusing on the integration of carbon fibers into two thermoplastic matrices: Polyamide with polyethylene terephthalate-glycol (PET-G) (PA). Examining the effects of these polymer matrices on the mechanical characteristics and microstructure of the resultant composite materials is the aim. Composite Fiber Co-Extrusion technology is used to produce samples containing both short and continuous carbon fibers, enabling a thorough evaluation of their performance.

Four different sample types are prepared—two for each polymer matrix—and tested under uniform 3D printing conditions to ensure consistency. The research involves analyzing the microstructure using microCT imaging, assessing mechanical strength through tensile tests, and evaluating thermal expansion properties relevant to aerospace applications. This research offers valuable insights for advancing composite materials used in aerospace and automotive industries, with a particular emphasis on their behavior in low-temperature environments, essential for extreme-condition applications. [8] The process starts by optimizing 3D printing technology, highlighting the need to upgrade equipment and adjust printing settings to improve the adaptability and performance of polymer composites. The review then presents innovative materials for 3D printing, such as new filaments, inks, photosensitive resins, and powders, explaining their distinctive properties and uses. With an emphasis on properties including thermal conductivity, electromagnetic interference shielding, biomedicine, self-healing capabilities, and environmental responsiveness, it delves deeper into the utilisation of 3D printing to produce functional polymer composites. The review also examines the effects of topological shape design and functional filler distribution on the characteristics of 3D printed goods. [9] fused filament fabrication (FFF) to produce three-dimensional (3D) printed components with graphene-based composite materials for space applications. Graphene composites are known for their remarkable qualities, such as radiation shielding, thermal resistance, and electrical conductivity, which make them ideal for multipurpose parts in space missions. The study tackles the difficulties of employing exfoliated graphene nanoplatelets (xGnP) composites and medium-density polyethylene (MDPE) in fused filament manufacture. The objective is to determine the FFF parameters required for effective 3D printing and improve the filament extrusion process. Tensile testing, electrical conductivity tests, and differential scanning calorimetry (DSC) are used to assess the material properties of the composites.

Through outgassing tests conducted under the AM0 sun spectrum, the study also evaluates the 3D-printed materials' compatibility with the space environment. The results demonstrate the possibility of FFF-based methods for producing MDPE/xGnP composites effectively and provide insightful information for in-space fabrication. [10] This discipline is being advanced in large part by 3D printing technology and the work of chemical and materials engineers who specialise in component design and fabrication. In particular, the utilisation of composite materials in fused deposition modelling is highlighted in this evaluation of the state of 3D printing today (FDM). 3D printing's history began in 1984 with the development of stereolithography, which signalled the beginning of the third Industrial Revolution and commercial additive manufacturing (AM). When Charles ("Chuck") Hull filed for a patent on the method in 1984, he came up with the term "stereolithography." Hull established 3D Systems, the first 3D printing business, in 1986 after creating this method, which allows the production of 3D things from layers of UV light-sensitive resin based on CAD software data. Scott Crump established Stratasys, the world's top 3D printing firm, after discovering FDM in 1988. FDM greatly shortens manufacturing cycle times by enabling the quick creation of 3D components from CAD designs. Molten material is forced into a print head nozzle during the process, depositing the material in horizontal layers as the head moves under computer control. Laminated Object Manufacturing (LOM), a technique developed by Helix in 1991, creates the object by cutting and adhering sheets of paper together. [11] the revolutionary effects of advanced composite materials and 3D printing technologies on a range of sectors. When it comes to mechanical, thermal, and electrical qualities, composite materials work better together in 3D printing than single-material composites making them highly advantageous in sectors such as aerospace, healthcare, and construction. The research highlights the innovative nature of this technology, examining its future possibilities. One key aspect investigated is the effect of print speeds on quality and efficiency. Fused Deposition Modeling (FDM) tests speeds ranging from 40 to 150 mm/s, assessing factors like layer adhesion and resolution. The study also delves into how different methods affect print speed, particularly in methods based on powder, such as Multi Jet Fusion (MJF) and Selective Laser Sintering (SLS), which use different

laserpower and material properties. These factors, including layer processing times, are crucial for optimizing print quality and production efficiency. The research emphasizes the need to balance speed, material properties, and desired print outcomes to enhance both product performance and manufacturing productivity.

The potential of composite material 3D printing is highlighted, underscoring its significance in commercial and industrial applications. As an additive manufacturing process, 3D printing differs from traditional subtractive manufacturing by building up materials layer by layer rather than removing material from solid blocks. The technology's ability to support rapid prototyping, complex designs, and personalized production has made it an essential tool in modern engineering and manufacturing. [12]Using 3D printing to create complexly shaped objects has become commonplace. Recent advancements in multi-material printing suggest that this technology could offer even greater design possibilities beyond just shape manipulation. In this study, we demonstrate how particle orientation can be controlled in a direct ink-writing process using anisotropic particles. We can direct particle alignment by applying modest magnetic fields to inks that contain magnetised stiff platelets. Furthermore, a two-component mixing system and multimaterial dispensers enable exact control over the local material composition. Using a five-dimensional design space, the suggested multimaterial magnetically assisted 3D printing (MM-3D printing) platform allows for the production of functional heterogeneous materials with intricate microstructures previously only found in biologically grown materials. [13]3D printing technology is increasingly being used across various fields of research and development. However, the potential of this transformative technology is still limited by the narrow selection of printable materials with a restricted range of physical and chemical properties.

There is growing interest in enhancing and broadening the properties of common printing materials by incorporating fillers with distinctive qualities or blending different materials to create high-performance composites. Several industries, including biological, mechanical, electrical, thermal, and optical devices, have already begun using these 3D printed composites. 3D printed composites are becoming more and more popular because of their capacity to create intricate structures, their affordable manufacturing costs, and the benefits of quick prototyping. This review focuses on current research that has improved the mechanical, electrical, thermal, optical, and biomaterial properties of basic 3D printable materials by adding nanoparticles, fibres, other polymers, or chemical processes to build composites. [14]These days, composite materials can be created by modern 3D printers as well as printed into components. At least two components with different qualities make up a composite material. It is a synthetically created heterogeneous material that usually consists of a matrix phase, which can be made of metal, ceramic, or polymer, and a reinforcement phase, which is normally rigid and offers resistance to external loads. In addition to providing reduced rigidity, the matrix is made to absorb the reinforcement, keeping it in place and distributing weight to the fibres. By combining materials with different properties, composites are created with enhanced characteristics. Common features of composite materials include reduced weight, increased strength, stiffness, toughness, and superior fatigue resistance. Certain composites also exhibit better properties like corrosion resistance, heat resistance, chemical stability, low thermal expansion, and reduced deformation when compared to conventionally uniform materials.

Therefore, composites can be described as efficient materials produced by combining reinforcement and matrix components in a way that they do not dissolve or become incompatible, preserving their individual properties while working together to offer improved performance. However, the downsides of Composite materials are more expensive and less recyclable. . Additionally, some composites may display anisotropic mechanical properties and degrade when exposed to high humidity and temperature over time. [15]Any 3D printing process must begin with a 3D digital model. There are several 3D design programmes that may be used to make this model. The model is "sliced" into layers in these programmes so that it can be sent to the 3D printer. Then, based on the model's shape and the printing technique, the printer applies material layer by layer. There are numerous 3D printing technologies available, and each one produces the finished product using a different set of materials and techniques. Various plastics, metals, ceramics, and sand powder are common materials; plastic, particularly ABS and PLA, is the most often used. 3D printing requires a variety of methods, procedures, and materials to produce the intended results, even though there isn't a single, universally applicable solution. Examples of such technologies include laser sintering, fused deposition modelling, stereolithography, digital light processing, and selective deposition lamination.

The Mark Two printer's usage of fused deposition modelling, or FDM, is the main topic of this introduction. One of the most straightforward and well-known 3D printing techniques, FDM, applies plastic filament layer by layer onto a platform after melting it with a hot extrusion head. [16]Rapid prototyping systems are increasingly popular technologies that allow using a range of materials to produce small batches and prototypes. Rapid developments targeted at lowering the cost of materials and equipment have resulted from the popularity of these technologies. One such popular technology is Fused Deposition Modeling (FDM), which is sometimes referred to as Fused Filament Fabrication (FFF) in open-source development. This process is frequently called Plastic Jet Printing (PJP), especially by companies such as 3D Systems and Stratasys. Machines made using this technology do have certain limitations, though. A major issue is that users are often required to purchase expensive proprietary filaments, typically only available from the machine's manufacturer.

These filaments are packaged with a chip containing a unique, non-computable ID, which the 3D printer reads to identify the type of material. The printer can then estimate the production volume possible with the specific coil based on the ID and other measurements. From the perspective of optimizing processing parameters, automatically adjusting material and nozzle temperatures, as well as the rate of filament deposition, based on coil ID recognition, offers significant advantages. However, the comparatively high monopolistic filament pricing, which are set by the machine manufacturers, limit the use of 3D printers and prevent a free market for semi-products made using FDM technology. The RepRap community, on the other hand, advocates for an open system that lets users use a large range of materials and filaments without any limitations imposed by the manufacturers of the machines. This method allows for the use of a wider variety of materials while lowering their cost.

The current study, which presents novel polymer composite materials, including polymers reinforced with natural fibres, was motivated by this idea. The primary advantages of these cutting-edge materials are their attractive look, special qualities, and the possibility of much cheaper costs, contingent on the percentage of natural content. [17] One of the most versatile additive manufacturing (AM) processes is direct ink writing (DIW), which may be used with a wide variety of materials. DIW is capable of producing complex 3D shapes by creating a paste with regulated flow characteristics. The creation of viscoplastic, self-healing inks that flow readily under shear and recover rapidly after deposition is one of its main obstacles. In order to develop inks that can handle a variety of materials, researchers look for adaptable techniques.

This work presents a DIW-applicable system based on the supramolecular interactions between triethanolamine and ammonium oleate. Rubber, plastic, ceramic, metal, and composites are just a few of the materials that can be printed utilising the shear-thinning DIW approach thanks to the ink system. More than 80% of the ink is solid, which inhibits the formation of porous structures and dimensional changes after printing. Multi-material sensors were successfully created using the established DIW approach for real-time health monitoring. This method might provide a fresh approach to creating 3D printing materials for a variety of useful uses. Because it does not require assembly, 3D printing, sometimes referred to as additive manufacturing, is essential to sustainable production because it reduces waste, energy use, and production time. It also makes it possible to mass customise complicated gadgets. Binder jetting, material jetting, vat photopolymerization, powder bed fusion, energy deposition, sheet lamination, fused deposition modelling (FDM), and DIW are some of the 3D printing methods that have been investigated. DIW is the most adaptable of them because of its. [18] We start by creating epoxy-based inks that have the rheological characteristics required for our 3D printing method in order to produce lightweight cellular composites. Epoxy resins are reactive substances that begin with low viscosity and progressively rise as the reaction proceeds at room temperature, in contrast to earlier ink formulations that solidify by gelation, drying, or spontaneous photopolymerization. To finish the polymerization process, these inks must be thermally cured for several hours at high temperatures (100–220°C). We created epoxy-based inks with and without highly anisotropic additives that have the proper viscoelasticity and long pot life. In particular, we used dimethyl methyl phosphonate, nano-clay platelets, and Epon 826 epoxy resin to manufacture the base inks (DMMP). The uncured ink exhibits shear thinning behaviour and a shear yield stress due to the rheology modifiers of the nano-clay platelets (1 nm thick; 100 nm long), while DMMP reduces the initial viscosity of the resin to allow for larger solids loading. Additionally, these chemicals aid in enhancing the cured epoxy matrix's mechanical qualities. After that, we added carbon fibres (10 µm in diameter; 220 µm average length) and silicon carbide whiskers (0.65 µm in diameter; 12 µm average length) to the basic formulation to create fiber-filled epoxy inks. During printing, the shear and extensional forces in the micronozzle cause these high aspect ratio fillers to align. [19] There is a growing sense of interdependence between advancements in 3D printing technology, materials science, and digital design tools. New materials, such as metals, composites, and advanced polymers, are improving the versatility and durability of 3D printed products.

These continuous technological advancements are not only expanding the possibilities of 3D printing but also increasing its accessibility for a larger group of people, fostering innovation and making people feel involved in these technical breakthroughs. Composites, due to their superior properties over traditional materials, are gaining significant attention across various industries. When two or more materials with dissimilar physical or chemical properties are combined characteristics, composites can exhibit enhanced features that individual components cannot. These benefits include increased durability, reduced weight, improved insulation, and greater chemical resistance. As a result, composites are frequently employed in domains like sports equipment, aerospace, automotive, and construction, offering long-lasting, low-maintenance, and high-performance solutions. The growing importance of composite materials in various sectors, driven by the push for efficiency and sustainability in production. For instance, carbon fibre-reinforced polymers (CFRPs) have revolutionized the manufacturing of airplane components, offering advantages like weight reduction, improved fuel efficiency, and lower carbon emissions. Similarly, composites are used in making lighter, more energy-efficient cars that meet stringent safety standards. Composites are also playing an important part in the field of

renewable energy , particularly in the creation of stronger, lighter wind turbine blades that maximize energy output while withstanding harsh environmental conditions. [20]

MATERIAL AND METHODS

Material

1. Printing Speed (mm/s)

One of the most important factors in the 3D printing process is the printing speed, or the pace at which material is extruded and placed onto the build platform. When it comes to composite materials, the printing speed has an impact on a number of final product characteristics, such as surface finish, layer adhesion, and the printed object's overall structural integrity. The standard unit of measurement for printing speed is millimetres per second (mm/s). A faster printing speed reduces the overall print time, making production more efficient. However, increasing the speed too much can lead to issues such as under-extrusion, poor layer bonding, or uneven deposition of the material. For composite materials, this is especially important because the filler material (e.g., carbon fibers or glass fibers) must be well-distributed and adequately bonded to the polymer matrix to achieve the desired mechanical properties. If the speed is too high, the material may not have enough time to properly bond between layers, resulting in weak spots or delamination. On the other hand, printing at a slower speed allows more time for each layer to adhere properly, ensuring a higher-quality surface finish and improved bonding. However, this increases the overall print time, which may be undesirable for high-volume production. Therefore, the optimal printing speed must balance print quality and time efficiency, and it typically depends on the part's complexity and the particular composite material being used and the desired mechanical properties.

2. Nozzle Temperature (°C)

One of the most crucial factors in 3D printing composite materials is nozzle temperature. The nozzle temperature determines how easily the material flows through the printer's extruder, affecting the consistency of the extrusion and the adhesion between layers. For composite filaments, which contain a mix of base polymers and reinforcing fillers, nozzle temperature is essential for guaranteeing that the polymer matrix and the filler material extrude smoothly and bond effectively. The temperature range for most composite filaments is between 190°C and 250°C, based on the kind of material being utilised. For example, PLA-based composite filaments typically require a lower temperature (around 190°C to 210°C), while filaments with higher-performance thermoplastics like ABS, PETG, or nylon require higher temperatures (210°C to 250°C). The polymer matrix might not melt if the nozzle temperature is set too low, leading to poor layer adhesion, incomplete extrusion, or even clogging of the nozzle. Conversely, excessively high temperatures can cause thermal degradation of both the base polymer and the filler material, which can result in weak parts, loss of strength, or unwanted surface defects. For composite materials with carbon fibers or glass fibers, controlling the nozzle temperature is especially important, as these fillers can degrade at high temperatures, reducing the material's reinforcing effect and impacting the final part's mechanical properties.

3. Filler Material (%)

The percentage of filler material in a composite filament has effects directly on the mechanical properties, such as strength, stiffness, wear resistance, and thermal conductivity. Fillers like carbon fibers, glass fibers, or metal powders are added to the polymer matrix to enhance its performance in specific applications. The filler material acts as reinforcement, providing strength and rigidity to the 3D-printed part, making it more suitable for demanding structural applications. In general, the more filler material present in the composite, the stronger and more rigid the printed part becomes. Carbon fiber-reinforced composites, for example, can achieve significant improvements in tensile strength, stiffness, and durability, making them ideal for aerospace, automotive, and industrial applications. However, the filler content must be carefully controlled. High filler percentages (e.g., 30% to 50%) can improve strength but may make the filament more difficult to print. High filler content can increase the viscosity of the material, causing extrusion problems such as clogging or inconsistent flow, and may also reduce the layer bonding, leading to weaker parts. The optimal filler material percentage depends on the desired mechanical properties and the specific application. For example, a 10% to 30% carbon fiber load typically offers a good balance between printability and material strength, whereas for more demanding applications requiring extreme strength, higher filler percentages may be required. It's essential to adjust other printing factors, like nozzle temperature and printing speed, to accommodate the increased viscosity and ensure proper material flow.

4. Tensile Strength (MPa)

The amount of force a material can bear before breaking when stretched is known as its tensile strength. It is among the most crucial mechanical characteristics of composite materials, especially when it

comes to applications, where structural integrity and load-bearing capacity are critical. Tensile strength is typically measured in megapascals (MPa) and varies widely based on the processing conditions and the composition of the material. For 3D-printed composite materials, tensile strength is influenced by several factors, including the base polymer, the type and percentage of filler material, the printing parameters, and post-processing techniques. In general, composite materials with higher filler content, such as carbon fiber or glass fiber, exhibit significantly higher tensile strength compared to unfilled polymers. Carbon fiber composites, for example, can achieve tensile strengths upwards of 100 MPa, which is far greater than that of typical 3D printing plastics like PLA or ABS. However, achieving high tensile strength requires more than just increasing the filler percentage. The printing process itself has a major impact on the printed part's ultimate mechanical characteristics. Proper layer bonding is essential for achieving the maximum tensile strength. The layers may not bond well if the printing speed is too high or the nozzle temperature is too low, creating weak spots that lower the part's tensile strength. Additionally, by strengthening the crystalline structure of the polymer matrix and strengthening the link between layers, post-processing methods like annealing or curing can increase tensile strength.

Machine Learning Algorithms

1. Linear Regression

Linear Regression (LR) is a popular statistical and machine learning method that is frequently used to simulate how variables relate to one another. Finding a positive or negative relationship between variables is the main goal of linear regression. One variable tends to rise along with the other in a positive connection. A negative association, on the other hand, occurs when one variable rises while the other falls. By measuring the statistically significant correlation between one or more variables, linear regression examines these relationships.

The variables in a linear regression model can be categorized into two types. The variable that is reliant on the by y , is the target value that the model seeks to predict or estimate. The independent variables, denoted by x_1, x_2, \dots, x_n , represent factors that influence or explain the behavior of the dependent variable. The model is referred to as "linear" because it assumes that in a two-dimensional graphic, the relationship between the independent and dependent variables can be represented by a straight line.

The simplest form of linear regression is represented by the equation:

$$y = c + mx$$

where m is the line's slope and c is the y -intercept. With the intercept c showing the value of y when x is zero and the slope m showing how much y varies for every unit change in x , this equation shows a straight-line relationship between x and y . The best-fitting line through a collection of data points is described by this equation.

In statistics, the linear regression equation is often written as:

$$y = \beta_0 + \beta_1 x_1$$

Here, β_0 is the intercept, and β_1 symbolises a basic linear regression model's slope. The coefficients β_0 and β_1 are estimated using statistical methods that reduce the discrepancy between the observed and anticipated values of y , like least squares.

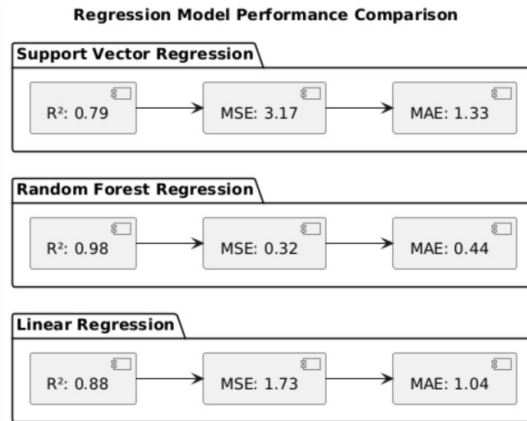
For more complex models, linear regression can involve multiple independent variables. When multiple predictors are included in the model, the general equation becomes:

$$y = \beta_0 + \beta_1 x_1 + \beta_2 x_2 + \dots + \beta_n x_n$$

This equation is known as multiple linear regression, where x_1, x_2, \dots, x_n are the independent variables, and each of the corresponding coefficients $\beta_1, \beta_2, \dots, \beta_n$ represents the change in y associated with a one-unit change in each of the respective predictors, assuming the other predictors are held constant.

Finding the best-fitting line (or hyperplane in the case of many variables) that reduces the error between the regression equation's projected values and the observed values of y is the aim of linear regression. A metric like the residual sum of squares (RSS), which is the sum of the squared discrepancies between the observed and predicted values, is commonly used to quantify this inaccuracy.

A basic statistical method for modelling and examining relationships between variables is linear regression. Whether it's used for predicting future values, estimating the strength of relationships, or understanding how different factors influence an outcome, linear regression provides valuable insights into the dynamics of various phenomena. By finding the optimal coefficients that most accurately depict how the dependent and independent variables are related, linear regression remains a core tool in both statistics and machine learning.



2. Random Forest Regression

Random forest regression (RFR) is a potent approach for predictive modelling in supervised machine learning. It belongs to the group of ensemble methods and is based on decision tree algorithms. Random forest essentially creates a collection of decision trees, each of which is trained on a distinct dataset subset. By averaging the outputs of these multiple trees, the random forest improves prediction accuracy while reducing the computational costs that would otherwise be associated with storing, training, and making predictions with numerous individual models. This makes random forest particularly effective for regression tasks, where it is commonly used to predict continuous values.

Building a "forest" of several decision trees is how the random forest method works. Every tree in the woodland is built independently, and the overall prediction of the random forest is the mean of all the forecasts provided by the individual trees. The trees themselves are constructed using the bagging technique, also known as bootstrapping, which involves training each tree on an arbitrary portion of the information. Because each tree in the forest is exposed to somewhat varied data, this technique helps to reduce variance and overfitting, improving the model's generalization ability.

In a random forest model, the decision trees are typically trained in parallel, making it a highly efficient process that can be distributed across multiple computing resources. This parallelism is a key advantage of random forest, as it allows the algorithm to take advantage of modern computational power, particularly when working with big datasets.

The output of the random forest regression model is produced by taking the average of each individual tree. Mathematically, this can be expressed as:

$$\text{Random Forest Prediction} = \frac{1}{K} \sum_{k=1}^K h_k(x)$$

where K is the overall quantity of separate regression trees constructed using the bootstrap samples, and $h_k(x)$ symbolises the forecast provided by the k -th regression tree for vector x as input. This aggregation of predictions from multiple trees helps to smooth out errors and make the final prediction more robust.

One of the key benefits of using random forests is that they are relatively quick to train, especially when in contrast to alternative machine learning models. This is mostly because of how parallel the decision trees in the forest. Additionally, random forests are known for their high accuracy, which stems from their ability to combine the predictions of many diverse models and minimize errors through averaging.

The mean squared error (MSE) for out-of-bag (OOB) data is a frequently used metric to assess a random forest model's effectiveness. The data points that are not chosen for a particular decision tree's bootstrap sample are known as "out-of-bag data," and they can be utilised to validate the model. The OOB dataset's MSE is determined by:

$$MSE_{OOB} = \frac{1}{n} \sum_{i=1}^n (y_i - \hat{y}_{i, OOB})^2$$

In this equation, y_i represents the true worth of the i -th data point, and $\hat{y}_{i, OOB}$ is the predicted value for the i -th data point based on the aggregation of all the decision trees in the forest. The sum of squared errors is averaged over all the data points in the OOB dataset to compute the MSE.

Another important metric for evaluating the random forest model is the coefficient of determination, often denoted as R^2 , which shows the extent to which the model can account for the variation in the data. For the OOB dataset, the R^2 value is calculated as:

$$R^2_{OOB} = 1 - \frac{MSC_{OOB}}{Var(y)}$$

where $Var(y)$ is the output parameter's overall variance. y . The R^2 value gives information about the percentage of the target variable's volatility that the model can account for. A higher R^2 shows that the model fits the data better, whereas a lower R^2 implies that a large portion of the variance cannot be explained by the model.

In summary, random forest regression is a highly effective and efficient ensemble method for predictive modeling. By building a forest of decision trees, it reduces overfitting and variance, leading to more accurate predictions. The use of bagging and parallelism enables random forest to train quickly and scale well with large datasets. With metrics like MSE and R^2 , the performance of a random forest model can be assessed, providing a reliable measure of its predictive power. Random forest continues to have gained popularity in machine learning applications because to their accuracy, efficiency, and resilience.

3. Support Vector Machines

Support Vector Machines (SVM) are robust and adaptable supervised machine learning algorithms that are frequently employed in regression, classification, and outlier identification. The SVM operates by determining the ideal hyperplane to divide data points into distinct classes. Maximizing the gap between data points of different classes while decreasing classification mistakes is its main goal. Finding the best hyperplane to partition the data points in a higher-dimensional space is the fundamental idea behind Support Vector Machines (SVM). This allows the data to be linearly separable when it is not in its original space.

Finding a hyperplane that maximises the distance between classes is the main goal of SVM. A hyperplane is a decision boundary that divides data points into two groups for a binary classification task. This would represent a line in two dimensions and a plane in three dimensions. SVM can function in any number of dimensions, though. The maximum margin, or the greatest distance between the hyperplane and the closest data points from each class, is what the SVM algorithm is intended to determine. Since they specify the location and direction of the hyperplane, these closest points—also referred to as support vectors—are crucial. Binary Classification

Let's consider the case of a binary classification problem where the goal is to classify data points into one of two classes: +1 and -1. Given a training dataset $\{(x^1, y^1), (x^2, y^2), \dots, (x^n, y^n)\}$, where x^i represents a feature vector and $y^i \in \{-1, +1\}$ is the corresponding class label, we aim to find a hyperplane defined by the equation:

$$w \cdot x + b = 0$$

where:

w is the weight vector perpendicular to the hyperplane.

b is the bias term.

x represents any point in the input space.

The objective is to maximize the margin $\frac{1}{||\omega||}$, which corresponds to minimizing $||\omega||$, subject to the constraint that each data point is correctly classified. For any data point x_i , the classification rule is:

$$y_i(w \cdot x_i + b) \geq 1$$

This ensures that all data points are correctly classified with a margin of at least 1 from the hyperplane. Thus, the optimization problem becomes:

$$\min_{w, b} \frac{1}{2} ||w||^2 \text{ subject to } y_i(w \cdot x_i + b) \geq 1, i = 1, 2, \dots, n$$

Kernel Trick

SVM use the kernel trick to translate data into a higher-dimensional space where it becomes linearly separable when the data is not linearly separable in its original space. SVM use a kernel function to calculate the transformation rather than doing so explicitly. $K(x, x')$ that calculates the higher – dimensional space's inner product

$$K(x, x') = \phi(x) \cdot \phi(x')$$

where $\phi(x)$ is the mapping function. Common kernel functions include:

Linear kernel: $K(x, x') = x \cdot x'$

Polynomial kernel: $K(x, x') = (x \cdot x' + c)^d$

Radial Basis Function (RBF) kernel: $K(x, x') = \exp(-\gamma ||x - x' ||)^2$

SVM is computationally efficient because of the kernel trick, which enables it to function in higher-dimensional spaces without explicitly calculating the converted coordinates.

Support Vectors Support vectors are the data points that are nearest to the hyperplane. These details are essential for establishing the optimal hyperplane. If the support vectors are removed, the position and orientation of the hyperplane could change significantly. Therefore, SVM focuses on these critical points to make decisions

about the hyperplane. In the equation for classification, When figuring out the best decision boundary, the support vectors are crucial.

SVM for Regression (SVR) In addition to classification, Regression issues, in which the objective is to predict a continuous output rather than classifying data points. This is called Support Vector Regression (SVR). In SVR, the objective is to find a function that preserves the margin between the data points and the regression line while departing from the actual values by no more than a given amount (or hyperplane in higher dimensions). The optimization problem for SVR is slightly different but follows the same principles of maximizing margins while minimizing errors.

RESULT AND DISCUSSION

Table 1: 3D printing of composite materials

Printing Speed (mm/s)	Nozzle Temperature (°C)	Filler Material (%)	Tensile Strength (MPa)
50	200	10	42
60	220	15	48
40	190	20	50
70	210	5	38
55	230	25	52
65	205	12	45
45	215	18	49
50	195	22	51
55	225	8	44
60	200	10	46
52	205	16	47
63	215	12	43
58	220	18	49
47	190	20	50
68	210	6	39
53	200	14	48
62	230	26	53
41	195	22	51
50	220	13	44
60	210	17	47
49	225	24	50
57	205	18	48
65	215	9	43
55	190	23	52
61	210	14	46
46	200	21	50
59	220	11	42
52	205	25	53
62	215	19	50
43	195	24	49

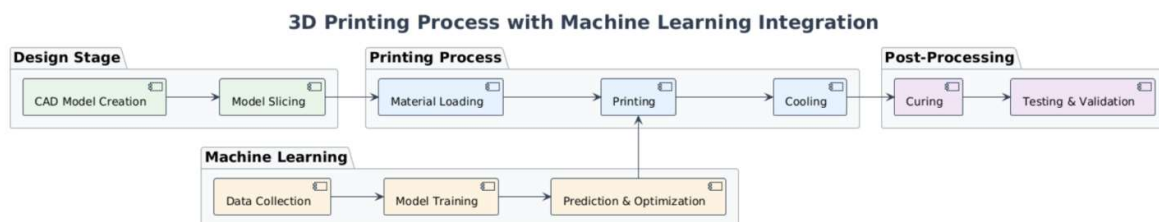
Table 1 presents data on the 3D printing of composite materials, detailing the effects of various printing parameters on the tensile strength of the printed material. The parameters include printing speed (in mm/s), nozzle temperature (in °C), filler material percentage, and the resulting tensile strength (in MPa). Each entry in the table represents a combination of these parameters, providing insights into how they influence the mechanical properties of the printed composites. Printing speed ranges from 40 to 70 mm/s, indicating a variability in the rate at which material is extruded during printing. Nozzle temperature varies between 190°C and 230°C, affecting the flow and bonding of the material. Filler material percentage, ranging from 5% to 26%, represents the proportion of reinforcement (such as carbon fiber, glass fiber, or other fillers) mixed with the base material, which significantly affects the composite's strength and durability. Finally, tensile strength values, which range from 38 MPa to 53 MPa, provide a measure of the material's resistance to breaking under tension. The data suggests a trend where higher filler material percentages tend to result in higher tensile strength, as seen with higher strength values like 53 MPa at 26% filler material. Similarly, nozzle temperature appears to influence tensile strength, with higher temperatures (such as 230°C) often leading to stronger materials.

However, the relationship between printing speed and tensile strength is less straightforward. In some cases, faster printing speeds like 70 mm/s result in lower tensile strength (38 MPa), while moderate speeds (e.g., 60 mm/s or 50 mm/s) tend to achieve relatively stronger materials. The table demonstrates how careful optimization of printing speed, nozzle temperature, and filler material percentage is crucial for achieving high-performance composite materials in 3D printing. The ability to adjust these parameters allows for the production of customized materials suited for a variety of applications, balancing factors like strength, printability, and material cost.

Table 2: Descriptive Statistics

	Printing Speed (mm/s)	Nozzle Temperature (°C)	Filler Material (%)	Tensile Strength (MPa)
count	30.000000	30.000000	30.000000	30.000000
mean	55.100000	208.833333	16.566667	47.300000
std	7.962628	11.867322	6.049698	3.992666
min	40.000000	190.000000	5.000000	38.000000
25%	50.000000	200.000000	12.000000	44.250000
50%	55.000000	210.000000	17.500000	48.000000
75%	60.750000	218.750000	21.750000	50.000000
max	70.000000	230.000000	26.000000	53.000000

Table 2 presents the descriptive statistics for the data on 3D printing of composite materials. It includes key statistical measures such as the count, mean, standard deviation (std), minimum (min), 25th percentile (25%), 50th percentile (median or 50%), 75th percentile (75%), and maximum (max) for the printing speed, nozzle temperature, filler material percentage, and tensile strength. The count for each variable is 30, indicating that the dataset consists of 30 observations for each of the four variables. The mean values show the average of each parameter: the mean printing speed is 55.1 mm/s, the mean nozzle temperature is 208.83°C, the mean filler material percentage is 16.57%, and the average tensile strength is 47.3 MPa. These values represent the central tendency of the data, offering an overview of typical conditions for the experiments. The standard deviation (std) quantifies the dispersion of the data from the mean. For example, the printing speed has a standard deviation of 7.96 mm/s, indicating a moderate variation around the average speed. Similarly, the standard deviation for tensile strength (3.99 MPa) indicates that while the values are somewhat clustered around the mean, there is notable variability in the material's strength across the dataset. The minimum (min) and maximum (max) values show the range of the data. The printing speed ranges from 40 mm/s to 70 mm/s, the nozzle temperature ranges from 190°C to 230°C, the filler material percentage ranges from 5% to 26%, and the tensile strength ranges from 38 MPa to 53 MPa. These extreme values help identify the boundaries within which the data points fall. The percentiles (25%, 50%, and 75%) provide additional insights into the distribution of the data. For instance, at the 25th percentile, the printing speed is 50 mm/s, while at the 75th percentile, it is 60.75 mm/s, indicating that a majority of the data points fall within this range. Similarly, the 50th percentile (median) for tensile strength is 48 MPa, suggesting that half of the tensile strengths are below this value, and half are above it.



Effect of Process Parameters

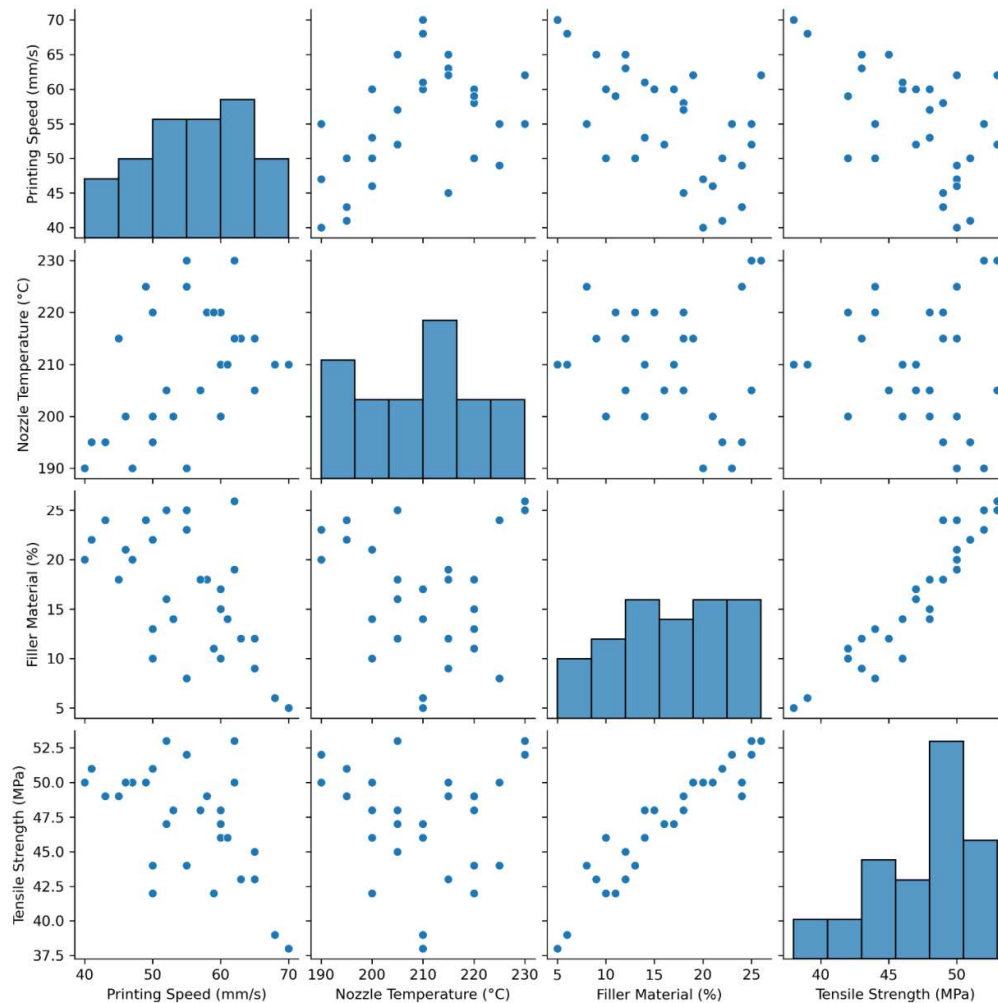


Fig 1: Scatter plot of the various 3D printing of composite materials process parameters

The figure 1 displays a Scatter plot of the various 3D printing of composite materials process parameters, which is a visual representation of the relationships between multiple variables: Printing Speed (mm/s), Nozzle Temperature ($^{\circ}\text{C}$), Filler Material (%), and Tensile Strength (MPa). Pairplots are useful for observing both individual distributions of variables and potential correlations between them. In the diagonal plots, histograms of each individual variable are shown, giving insight into their distributions. The Printing Speed histogram indicates a relatively uniform distribution between 40 mm/s and 70 mm/s. The Nozzle Temperature distribution has a central tendency around 210°C , with a slightly higher frequency of temperatures between 200°C and 220°C . The Filler Material histogram reveals a range of values between 5% and 26%, with a higher concentration around 20%. Lastly, the Tensile Strength distribution is somewhat symmetric, ranging from 38 MPa to 53 MPa, with a clustering of values between 44 MPa and 51 MPa. Off-diagonal plots display scatter plots that reveal the relationships between pairs of variables. Notably, there seems to be a moderate positive correlation between Filler Material (%) and Tensile Strength (MPa). As the filler material percentage increases, tensile strength tends to rise as well, which is consistent with the general expectation that higher reinforcement improves the mechanical properties of composites. However, the relationship between Printing Speed and Tensile Strength does not show a clear trend, indicating that printing speed may not have a strong or consistent effect on tensile strength. Similarly, the correlation between Nozzle Temperature and Tensile Strength is less evident, although a slight positive trend is observable in some parts of the scatter plot.

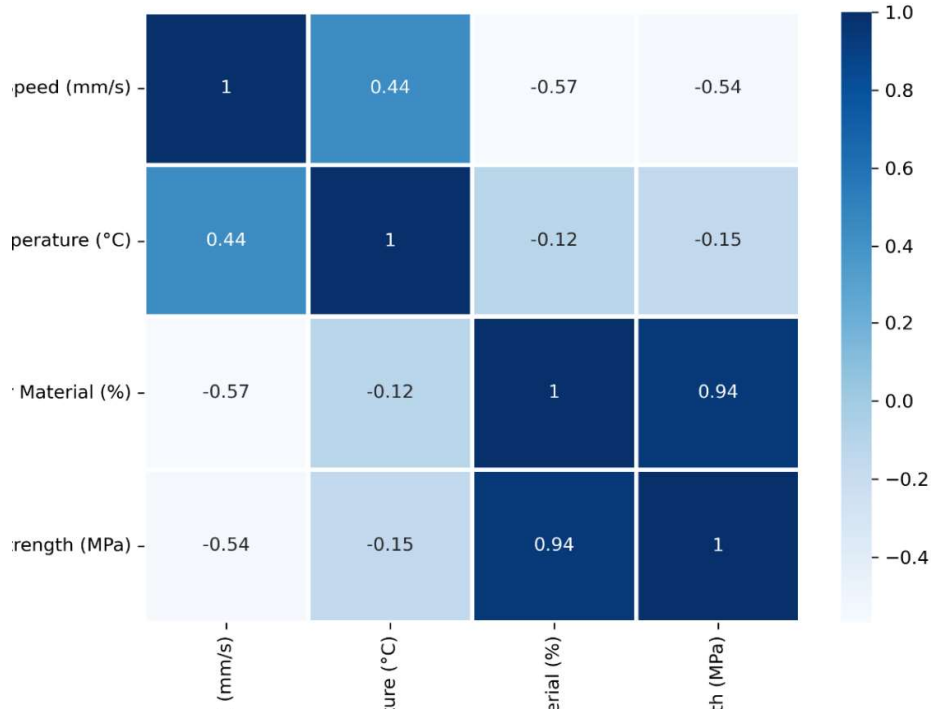


Fig 2: Correlation heatmap between the process parameters and the responses

The figure 2 represents a correlation heatmap that quantifies the strength and direction of linear relationships between the process parameters (Printing Speed, Nozzle Temperature, Filler Material) and the response variable (Tensile Strength). A strong positive association is indicated by a correlation coefficient close to 1, a strong negative relationship is shown by a correlation coefficient close to -1, and little to no correlation is suggested by a correlation coefficient near 0. The heatmap's colour gradient vividly highlights the strength and direction of these relationships.

Filler Material and Tensile Strength: The strongest positive correlation in the dataset is observed between Filler Material (%) and Tensile Strength (MPa), with a correlation coefficient of 0.94. This indicates a near-linear relationship where increasing the percentage of filler material significantly improves the tensile strength. This is expected in composite materials, as fillers often enhance mechanical properties.

Printing Speed and Tensile Strength: A moderately strong negative correlation (-0.54) exists between Printing Speed (mm/s) and Tensile Strength (MPa). This suggests that higher printing speeds may compromise the tensile strength, likely due to reduced layer adhesion or improper material deposition at higher speeds.

Nozzle Temperature and Tensile Strength: The correlation between Nozzle Temperature (°C) and Tensile Strength (MPa) is weakly negative (-0.15), suggesting that nozzle temperature has minimal direct influence on tensile strength within the range considered. However, it may interact with other factors, such as filler material or speed, in more complex ways.

Printing Speed and Nozzle Temperature exhibit a moderate positive correlation (0.44), implying that higher speeds may often coincide with elevated nozzle temperatures, potentially due to process optimization settings. A significant negative correlation (-0.57) is observed between Printing Speed and Filler Material, indicating that lower printing speeds are often paired with higher filler material percentages, which may be necessary to maintain quality and precision during the printing process. Nozzle Temperature and Filler Material show a weak negative correlation (-0.12), indicating minimal interaction between these parameters.

Linear Regression (LR)

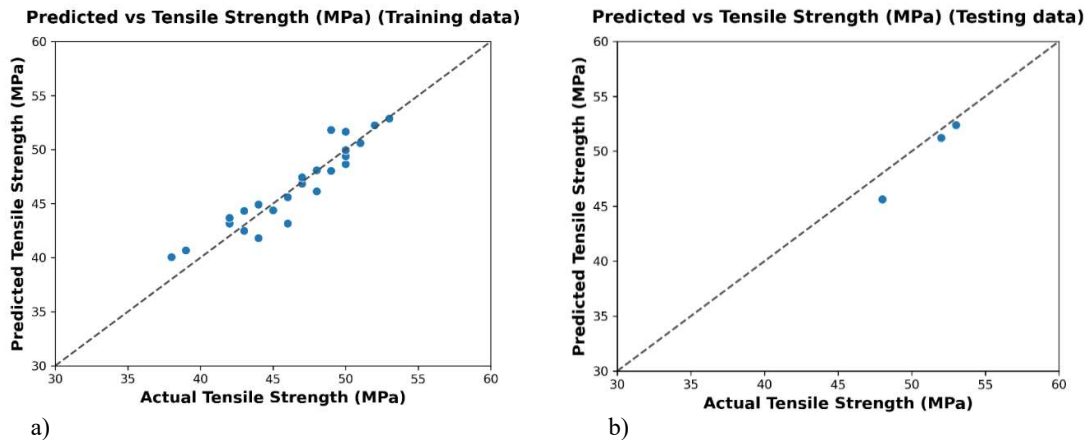


Fig 3. Predictive performance of the linear regression predictive model in 3D printing of composite materials (a) train; (b) test.

The provided scatter plot in Figure 3(a) illustrates the ability of a linear regression model to predict trained to estimate the Tensile Strength (MPa) of composite materials based on the 3D printing process parameters. The y-axis shows the projected tensile strength values produced by the model, and the x-axis shows the actual tensile strength values from the training dataset. The ideal situation, in which the anticipated values exactly match the actual values, is shown by the diagonal dashed line. Prediction Accuracy: The majority of data points closely match the diagonal line, suggesting that the model's predictions and the training set's actual tensile strength values agree quite well. Model Fit: The consistent distribution of points around the diagonal suggests minimal bias in the predictions, with no significant overprediction or underprediction across the tensile strength range. Outliers: There appear to be a few points slightly deviating from the diagonal line, which could indicate minor discrepancies in the model's fit for certain data points.

A linear regression model used to forecast the tensile strength of 3D-printed composite materials during the "b" test is shown in the scatter plot that is provided. The y-axis displays the anticipated tensile strength, and the x-axis displays the actual tensile strength (in MPa). The ideal situation, where forecasts and actual values are exactly the same, is shown by the dashed diagonal line. Given that the majority of the data points are located along the diagonal line, it is clear from the plot that the linear regression model produces predictions that are reasonably accurate. This implies that the model accurately depicts the relationship between the tensile strength and the input parameters (such as temperature, printing speed, and material composition). However, some deviations from the ideal line are visible, indicating prediction errors. These errors could be due to inherent variability in the 3D printing process, unaccounted nonlinear interactions, or limitations of the linear regression model in handling complex relationships. The model's predictive accuracy can be quantified using metrics like the R-squared value or Mean Squared Error. While linear regression is useful for establishing a basic relationship, improvements could be achieved by exploring nonlinear models or incorporating additional features to capture complex dependencies in the data.

Random Forest Regression (RFR)

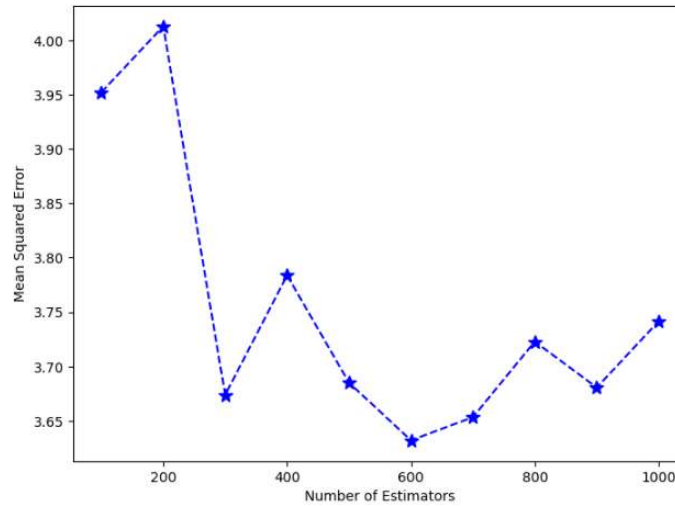


Fig 4:Effect of number of repressor in random forest regression on Number of Estimators vs Mean Squared Error

Figure 4 illustrates the relationship between the number of estimators in a random forest regression model as well as the projections' Mean Squared Error (MSE). The y-axis shows the Mean Squared Error, which calculates the average squared difference between predicted and actual values, while the x-axis shows the number of estimators (decision trees) in the random forest, which ranges from roughly 200 to 1000, with values spanning approximately 3.65 to 4.0. A noticeable spike in MSE occurs when using 200–300 estimators, reaching its highest value of around 4.0. Beyond this peak, the error decreases sharply, dropping to approximately 3.67 when the number of estimators reaches 400. After 400 estimators, the error rate stabilizes, showing only minor fluctuations. The minimum MSE, about 3.65, is observed near 600 estimators, indicating the best model performance. Adding more than 600 estimators results in negligible improvements, with only slight variations in the error rate. These findings suggest that while fewer estimators (200–300) result in higher error rates, increasing the number to around 600 optimizes performance. Adding more estimators beyond this point offers diminishing returns in reducing the error.

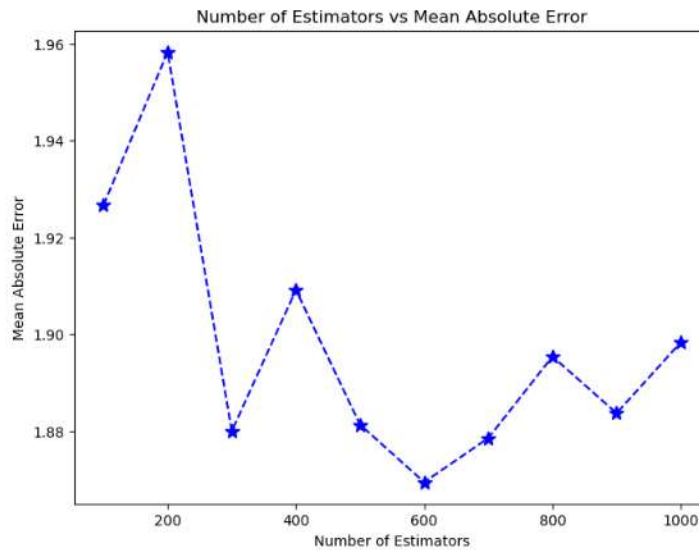


Fig 5:Effect of number of repressor in random forest regression on Number of Estimators vs Mean Absolute Error

Figure 5 presents a graph depicting the relationship between the number of estimators in a random forest regression model and the Mean Absolute Error (MAE). The analysis highlights several key observations X-axis: Number of estimators, ranging from approximately 100 to 1000. Y-axis: Mean Absolute Error values, spanning roughly from 1.87 to 1.96. Initial Spike: A sharp increase in error, peaking at about 1.96 around 200 estimators. Subsequent Drop: A notable decrease to approximately 1.88 at 300 estimators. Secondary Peak: A smaller rise in error, reaching around 1.91 near 400 estimators. Stabilization: Post 600 estimators, the error stabilizes with minor fluctuations. Optimal Point: The lowest MAE, about 1.87, occurs around 600 estimators. This trend aligns closely with the behavior observed in the Mean Squared Error (MSE) plot (Figure 4), indicating consistency across different error metrics. The findings suggest that utilizing approximately 600 estimators yields optimal performance, as increasing the number of trees beyond this threshold does not significantly enhance the model's accuracy. The parallel patterns between MAE and MSE further corroborate the robustness of these results across various error measurements. These observations are consistent with findings in the literature, where the performance of random forests tends to stabilize or even degrade slightly beyond a certain number of estimators. For instance, a study on the consistency of random forests discusses how the model's error metrics behave with an increasing number of trees, emphasizing the importance of selecting an optimal number of estimators to balance performance and computational efficiency.

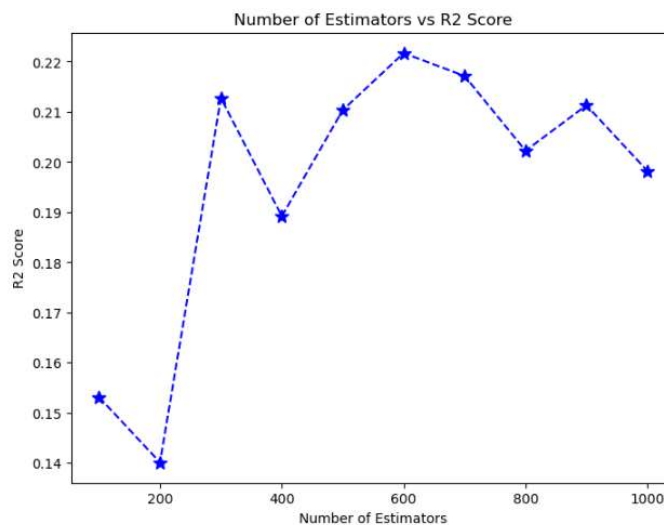


Fig 6:Effect of number of repressor in random forest regression on Number of Estimators vs R2 Score

Figure 6 depicts the relationship between the number of estimators in a random forest regression model and the R^2 (R-squared) score, which indicates how well the model explains the variance in the dependent variable. Key takeaways from the graph are The R^2 score begins at around 0.15 with 100 estimators. A slight decrease is observed, reaching approximately 0.14 near 200 estimators. A significant improvement follows between 200 and 300 estimators, with the R^2 score rising to about 0.21. Between 300 and 600 estimators, the score fluctuates moderately. Peak performance is observed at roughly 600 estimators, with an R^2 score of about 0.22. Beyond 600 estimators, the score gradually declines with minor variations, stabilizing at approximately 0.20 by 1,000 estimators. This trend indicates the model's explanatory power is optimized near 600 estimators, consistent with observations from the MSE and MAE plots (Figures 4 and 5). However, the modest maximum R^2 score of 0.22 suggests that a substantial portion of variance remains unexplained, pointing to potential complexities in the relationship between features and the target variable or the need for additional features to enhance predictive performance.

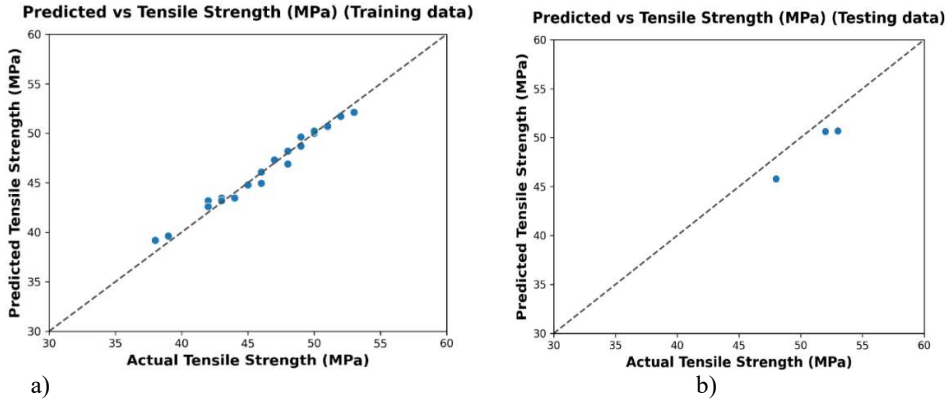


Fig 7: Predictive performance of the random forest regression predictive model in 3D printing of composite materials a) train b) test

The figure 7 demonstrates the predictive performance of a Random Forest Regression model applied to the a) training data for estimating the tensile strength of composite materials used in 3D printing. The scatter plot compares the predicted tensile strength (y-axis) with the actual tensile strength (x-axis), measured in megapascals (MPa). A data point in the training set is represented by each blue dot, which shows the correlation between the expected and actual values. The ideal prediction situation, where the projected values exactly match the actual values, is represented by the dashed diagonal line. The data points closely cluster around this diagonal, indicating that the model performs well on the training set with little error. This kind of performance suggests that the dataset's fundamental patterns and relationships are adequately captured by the Random Forest Regression model. This strong correlation in training data indicates a well-trained model; however, further evaluation using validation or testing data is necessary to guarantee the model's successful generalisation to unknown data. The figure underscores the potential of Random Forest Regression for accurately modeling and predicting material properties in 3D printing applications.

b) Testing data for estimating the tensile strength of composite materials in 3D printing. The scatter plot compares the predicted tensile strength (y-axis) with the actual tensile strength (x-axis), measured in megapascals (MPa). In the testing dataset, each blue dot represents a data point. The ideal situation, where projected values precisely match the actual tensile strength, is represented by the dotted diagonal line. The majority of the data points in this picture are around the diagonal, indicating that the model does a respectable job on the test data. However, the small number of points indicates a limited test set, which may constrain the evaluation of the model's generalizability. It appears that the model maintains predicted accuracy even when dealing with unknown data because the data points are well aligned with the diagonal. However, any observed deviations highlight areas for further improvement in modeling or additional feature refinement. This evaluation is critical to confirm the Random Forest model's robustness and effectiveness in predicting material properties for 3D printing applications.

Support Vector Machines (SVM)

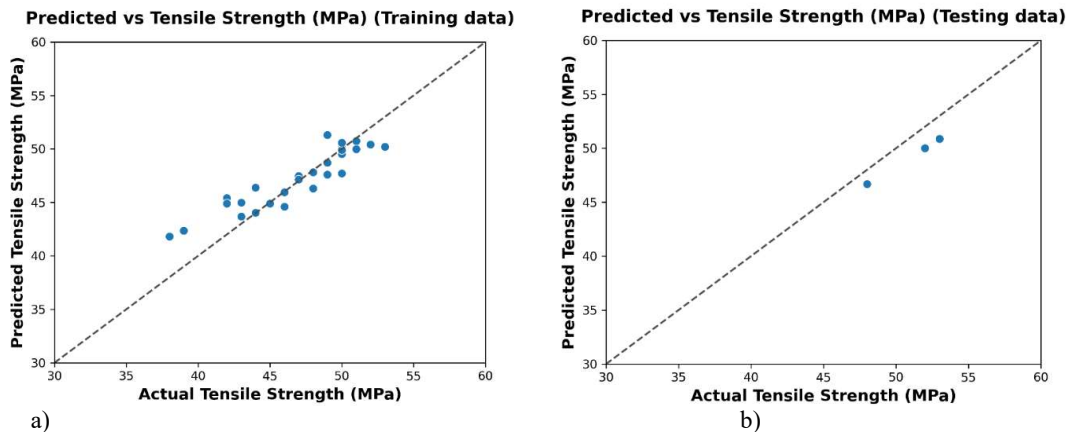


Fig 8: Predictive performance of the Support Vector Machines predictive model in 3D printing of composite materials a) train b) test

The figure 8 shows the predictive performance of a Support Vector Machines (SVM) regression model applied to the training data for predicting the tensile strength of composite materials used in 3D printing. The scatter plot compares the predicted tensile strength (y-axis) with the actual tensile strength (x-axis), both measured in megapascals (MPa). Every blue dot represents a training set data point. The ideal situation, in which the anticipated values precisely match the actual values, is shown by the dashed diagonal line. The majority of the data points are grouped together around this line, suggesting that the SVM regression model fits the training data well and operates accurately. The graphic indicates that the intricate correlations between characteristics and tensile strength in the training dataset are well captured by the SVM model. To verify the model's capacity to generalise to novel, untested data, its actual performance should also be evaluated on a different testing dataset. This strong alignment between predictions and actual values highlights the potential of SVM regression for precise modeling of material properties in 3D printing.

b) Testing data for scatter plot comparing predicted versus actual tensile strength values (measured in MPa) for what appears to be testing data from a Support Vector Machine (SVM) model used in 3D printing of composite materials. A diagonal dashed line in the plot signifies perfect prediction (where predicted values exactly match actual values). This line appears to have a number of blue data points strewn about it, which are the model's forecasts, compared to the actual measured tensile strength values. The actual tensile strength ranging from approximately 30 to 60 MPa, while the y-axis shows the predicted tensile strength over the same range. The data points seem to cluster fairly close to the diagonal line, suggesting reasonable predictive performance of the SVM model, though there is some visible scatter indicating prediction errors. Looking at the distribution of points, the model appears to have made predictions in the range of about 40-50 MPa. Most points fall near but not exactly on the diagonal line, indicating that while the model has captured the general relationship between input features and tensile strength, it's not perfect in its predictions. This type of visualization is commonly used to evaluate regression model performance, with points closer to the diagonal line indicating better predictions. The relatively tight clustering of points around the line suggests this SVM model has achieved reasonable accuracy in predicting the tensile strength of 3D printed composite materials.

Table 3: Regression Model Performance Metrics (Training Data)

	Data	Symbol	Model	R2	EVS	MSE	RMSE	MAE	MaxError	MSLE	MedAE
1	Training	LR	Linear Regression	0.88397	0.88397	1.73E+00	1.32E+00	1.04E+00	2.82E+00	8.18E-04	9.17E-01
2	Training	RFR	Random Forest Regression	0.97845	0.97845	3.21E-01	5.67E-01	4.43E-01	1.20E+00	1.58E-04	3.10E-01
3	Training	SVR	Support Vector Regression	0.787566	0.794306	3.17E+00	1.78E+00	1.33E+00	3.81E+00	1.54E-03	1.01E+00

The regression model performance metrics for training data, as summarized in Table 3, provide insights into the comparative effectiveness of three models: Linear Regression (LR), Random Forest Regression (RFR), and Support Vector Regression (SVR). These metrics, including R^2 , Explained Variance Score (EVS), Mean Squared Error (MSE), Root Mean Squared Error (RMSE), Mean Absolute Error (MAE), Maximum Error, Mean Squared Log Error (MSLE), and Median Absolute Error (MedAE), reflect the models' predictive capabilities. Among the models, RFR demonstrated the highest performance, achieving an R^2 of 0.97845 and an EVS of 0.978465, demonstrating its capacity to roughly explain 97.8% of the variance in the data. It also recorded the lowest MSE (0.321), RMSE (0.567), and MAE (0.443), highlighting its precision and minimal prediction errors. Additionally, RFR's MaxError and MedAE were notably low at 1.20 and 0.31, respectively, confirming its robustness and consistency. LR showed moderate performance, with an R^2 of 0.88397 and an equivalent EVS. While it performed adequately in minimizing errors, its MSE (1.73), RMSE (1.32), and MAE (1.04) were higher than those of RFR, indicating less accurate predictions. Nonetheless, LR maintained reasonable error margins and performed reliably overall. In contrast, SVR had the weakest performance among the three models, with an R^2 of 0.787566 and an EVS of 0.794306. Its MSE (3.17), RMSE (1.78), and MAE (1.33) were significantly higher, indicating larger prediction deviations. SVR also exhibited the highest MaxError (3.81) and MSLE (0.00154), reflecting its comparatively lower accuracy and consistency. RFR outperformed LR and SVR across most metrics, demonstrating its superior ability to model and predict the training data accurately, followed by LR with moderate performance and SVR with relatively lower predictive efficiency.

Table 4: Regression Model Performance Metrics (Testing Data)

	Data	Symbol	Model	R2	EVS	MSE	RMSE	MAE	MaxError	MSLE	MedAE
1	Test	LR	Linear Regression	0.534037	0.865613	2.17E+00	1.47E+00	1.24E+00	2.36E+00	9.25E-04	7.62E-01
2	Test	RFR	Random Forest Regression	0.140123	0.961924	4.01E+00	2.00E+00	1.96E+00	2.31E+00	1.57E-03	2.21E+00
3	Test	SVR	Support Vector Regression	0.267021	0.972702	3.42E+00	1.85E+00	1.81E+00	2.13E+00	1.28E-03	2.00E+00

Table 4 presents the regression model performance metrics for testing data, comparing Linear Regression (LR), Random Forest Regression (RFR), and Support Vector Regression (SVR) based on several key indicators: R^2 , Explained Variance Score (EVS), Mean Squared Error (MSE), Root Mean Squared Error (RMSE), Mean Absolute Error (MAE), Maximum Error, Mean Squared Log Error (MSLE), and Median Absolute Error (MedAE). These metrics provide valuable insights into the models' generalization and predictive accuracy on unseen data. Among the models, LR demonstrated relatively better performance on testing data, achieving an R^2 of 0.534037 and an EVS of 0.865613. Its MSE (2.17), RMSE (1.47), and MAE (1.24) indicate reasonable prediction accuracy, although these values highlight higher error margins compared to training data performance. The MaxError (2.36) and MedAE (0.762) suggest LR maintained consistency in prediction, performing better than RFR and SVR on certain error metrics. SVR achieved an intermediate level of performance, with an R^2 of 0.267021 and an EVS of 0.972702. Its MSE (3.42), RMSE (1.85), and MAE (1.81) were higher than LR, indicating greater prediction errors. However, SVR had the lowest MaxError (2.13), reflecting its relative ability to limit extreme deviations. Despite this, the MedAE (2.00) indicates a lack of precision in overall prediction consistency compared to LR. RFR underperformed on testing data with an R^2 of 0.140123 and an EVS of 0.961924. Its MSE (4.01), RMSE (2.00), and MAE (1.96) were the highest among the models, indicating significant errors in prediction. Furthermore, the MaxError (2.31) and MedAE (2.21) highlight its lower accuracy and consistency. LR exhibited the best generalization among the models, followed by SVR, while RFR struggled with testing data, underscoring the challenges of maintaining training performance on unseen data.

CONCLUSION

3D-printed composite materials through various regression modeling approaches. The research investigated the relationships between key process parameters (printing speed, nozzle temperature, and filler material percentage) and their impact on tensile strength, utilizing models of Support Vector Regression (SVR), Random Forest Regression (RFR), and Linear Regression (LR). The analysis revealed strong correlations between process parameters and tensile strength, particularly highlighting a significant positive correlation (0.94) between filler material percentage and tensile strength. This finding confirms that higher filler content generally leads to improved mechanical properties in composite materials. Conversely, printing speed showed a moderate negative correlation (-0.54) with tensile strength, suggesting that faster printing speeds may compromise material strength, likely due to reduced layer adhesion. In terms of model performance on training data, Superior prediction performance was shown by the Random Forest Regression model with an R^2 value of 0.97845 and the lowest error metrics (MSE: 0.321, RMSE: 0.567, MAE: 0.443). This was followed by Linear Regression (R^2 : 0.88397) and Support Vector Regression (R^2 : 0.787566). However, when tested on unseen data, the models showed different behavior patterns. Linear Regression exhibited better generalization with an R^2 of 0.534037 and lower error metrics compared to both RFR and SVR on the test dataset. This unexpected shift in performance highlights the importance of model validation and the challenges of maintaining predictive accuracy across different datasets. The optimization analysis of the Random Forest model revealed that approximately 600 estimators provided the optimal balance between model complexity and prediction accuracy. This was evidenced by the stabilization of both Mean Squared Error and Mean Absolute Error metrics beyond this point, suggesting that additional complexity offers diminishing returns in model performance. These findings have significant implications for the 3D printing industry, particularly in the manufacturing of composite materials. The research demonstrates that while complex models like Random Forest Regression may excel in capturing intricate relationships within training data, simpler models like Linear Regression might offer more robust and generalizable predictions in practical applications. This suggests that when implementing predictive models in real-world manufacturing scenarios, the choice of model should consider not only training performance but also generalization capability and computational efficiency. Subsequent investigations may examine the incorporation of extra process parameters, investigation of non-linear relationships between variables, and the creation of hybrid modelling techniques that blend the strengths of different regression techniques. Furthermore, the study highlights the need for larger datasets and more sophisticated cross-

validation techniques to improve model robustness and reliability in predicting the mechanical characteristics of composite materials manufactured using 3D.

REFERENCES

1. Daniela, Tichá., Juraj, Tomášik., Eubica, Oravcová., Andrej, Thurzo. (2024). Three-Dimensionally-Printed Polymer and Composite Materials for Dental Applications with Focus on Orthodontics. *Polymers*, 16(22), 3151-3151. doi: 10.3390/polym16223151.
2. Ye-eun, Park., Sunhee, Lee. (2024). Characterization of PLA/LW-PLA Composite Materials Manufactured by Dual-Nozzle FDM 3D-Printing Processes. *Polymers*, 16(20), 2852-2852. doi: 10.3390/polym16202852.
3. Dachepalli V (2023). Machine Learning and Grey Relational Analysis: A Hybrid Approach to Fraud Detection in Shipping Payments. *J Comp Sci Appl Inform Technol*. 8(1): 1-8
4. S., Thamizh, Selvan., M, Mohandass., V.S., Senthil, Kumar. (2024). Pattern optimization for 3D printing of composite filament materials with natural fibers and polylactic acid. *Proceedings Of The Institution Of Mechanical Engineers, Part E: Journal Of Process Mechanical Engineering*, doi: 10.1177/09544089241281436.
5. Sridhar Kakulavaram. (2022). Life Insurance Customer Prediction and Sustainability Analysis Using Machine Learning Techniques. *International Journal of Intelligent Systems and Applications in Engineering*, 10(3s), 390 –. Retrieved from <https://ijisae.org/index.php/IJISAE/article/view/7649>
6. Arif, M., Abdullah., Martin, L., Dunn., Kai, Yu. (2024). Robotic 3D Printing of Continuous Fiber Reinforced Thermoset Composites. *Advanced materials & technologies*, doi: 10.1002/admt.202400839.
7. Arslan, KAPTAN., Fuat, Kartal. (2024). A review on integration of carbon fiber and polymer matrix composites in 3D printing technology. *International advanced researches and engineering journal*, doi: 10.35860/iaorej.1484042.
8. Emanuela, Tamburri., Luca, Montaina., Francesca, Pescosolido., Carcione, Rocco., Silvia, Battistoni. (2024). 3D Extrusion and Stereolithography Printing Methods for Producing Multifunctional Polymer Composites. *Macromolecular Symposia*, 413(4) doi: 10.1002/masy.202400030.
9. Null, Author_Id., Null, Author_Id., Caleb, Oliver, Bedsole., Zhijian, Pei., Brian, D., Shaw., Null, Author_Id., M.E., Castell□Perez. (2024). Effects of Incorporating Ionic Crosslinking on 3D Printing of Biomass–Fungi Composite Materials. *Biomimetics*, 9(7), 411-411. doi: 10.3390/biomimetics9070411.
10. Mittapally R (2023). Evaluating Business Intelligence Alternatives: COPRAS vs Traditional Models in MicroStrategy. *J Comp Sci Appl Inform Technol*. 8(1): 1-9.
11. Karel, Dvorak., Lucie, Zárybnická., Radek, Ševčík., Michal, Vopalensky., Irena, Adámková. (2024). 3D composite printing: study of carbon fiber incorporation to different construction thermoplastic matrices in regard to dilatation characteristics. *Rapid Prototyping Journal*, doi: 10.1108/rpj-12-2023-0450.
12. Tengbo, Ma., Yali, Zhang., Kunpeng, Ruan., Hua, Guo., Mukun, He., Xuetao, Shi., Yongqiang, Guo., Jie, Kong., Junwei, Gu. (2024). Advances in <sc>3D</sc> printing for polymer composites: A review. *InfoMat*, doi: 10.1002/inf2.12568.
13. Susanna, Laurenzi., Federica, Zaccardi., Elisa, Toto., M., Gabriella, Santonicola., Sabina, Botti., Tanya, Scalia. (2024). Fused Filament Fabrication of Polyethylene/Graphene Composites for In-Space Manufacturing. *Materials*, doi: 10.3390/ma17081888.
14. Blanco, Ignazio. "The use of composite materials in 3D printing." *Journal of Composites Science* 4, no. 2 (2020): 42.
15. Ballamudi, S. "Interleaved Feature Extraction Model Bridging Multiple Techniques for Enhanced Object Identification" *Journal of Artificial Intelligence and Machine Learning*, 2023, vol. 1, no. 2, pp. 1-7. doi: <https://doi.org/10.55124/jaim.v1i2.253>
16. Alarifi, Ibrahim M. "Revolutionising fabrication advances and applications of 3D printing with composite materials: a review." *Virtual and Physical Prototyping* 19, no. 1 (2024): e2390504.
17. Kokkinis, Dimitri, Manuel Schaffner, and André R. Studart. "Multimaterial magnetically assisted 3D printing of composite materials." *Nature communications* 6, no. 1 (2015): 8643.
18. Kalsoom, Umme, Pavel N. Nesterenko, and Brett Paull. "Recent developments in 3D printable composite materials." *RSC advances* 6, no. 65 (2016): 60355-60371.
19. Bárník, František, Milan Vaško, Milan Sága, MariánHandrik, and AlžbetaSapietová. "Mechanical properties of structures produced by 3D printing from composite materials." In *MATEC Web of Conferences*, vol. 254, p. 01018. EDP Sciences, 2019.
20. Velu, Rajkumar, Felix Raspall, and SaratSingamneni. "3D printing technologies and composite materials for structural applications." In *Green composites for automotive applications*, pp. 171-196. Woodhead Publishing, 2019.

21. Šafka, Jiří, Michal Ackermann, JiříBobek, Martin Seidl, JiříHabr, and LubošBěhálek. "Use of composite materials for FDM 3D print technology." In *Materials science forum*, vol. 862, pp. 174-181. Trans Tech Publications Ltd, 2016.
22. Yang, Guiyan, Youyi Sun, Mengru Li, KangtaiOu, Jiang Fang, and Qiang Fu. "Direct-ink-writing (DIW) 3D printing functional composite materials based on supra-molecular interaction." *Composites Science and Technology* 215 (2021): 109013.
23. Compton, Brett G., and Jennifer A. Lewis. "3D□printing of lightweight cellular composites." *Advanced materials* 26, no. 34 (2014): 5930-5935.
24. Dudek, P. F. D. M. "FDM 3D printing technology in manufacturing composite elements." *Archives of metallurgy and materials* 58, no. 4 (2013): 1415-1418.